

# CellMix: A General Instance Relationship based Method for Data Augmentation Towards Pathology Image Analysis

Tianyi Zhang<sup>1\*</sup> Zhiling Yan<sup>1\*</sup> Chunhui Li<sup>2</sup> Nan Ying<sup>1</sup> Yanli Lei<sup>1</sup>  
Yunlu Feng<sup>3</sup> Yu Zhao<sup>4</sup> Guanglei Zhang<sup>1†</sup>

<sup>1</sup>School of Biological Science and Medical Engineering, Beihang University

<sup>2</sup>School of Artificial Intelligence, Nanjing University

<sup>3</sup>Department of Gastroenterology, Peking Union Medical College Hospital

<sup>4</sup>Department of Pathology, Peking Union Medical College Hospital

## Abstract

Pathology image analysis crucially relies on the availability and quality of annotated pathological samples, which are very difficult to collect and need lots of human effort. To address this issue, beyond traditional preprocess data augmentation methods, mixing-based approaches are effective and practical. However, previous mixing-based data augmentation methods do not thoroughly explore the essential characteristics of pathology images, including the local specificity, global distribution, and inner/outer-sample instance relationship. To further understand the pathology characteristics and make up effective pseudo samples, we propose the CellMix framework with a novel distribution-based in-place shuffle strategy. We split the images into patches with respect to the granularity of pathology instances and do the shuffle process across the same batch. In this way, we generate new samples while keeping the absolute relationship of pathology instances intact. Furthermore, to deal with the perturbations and distribution-based noise, we devise a loss-drive strategy inspired by curriculum learning during the training process, making the model fit the augmented data adaptively. It is worth mentioning that we are the first to explore data augmentation techniques in the pathology image field. Experiments show SOTA results on 7 different datasets. We conclude that this novel instance relationship-based strategy can shed light on general data augmentation for pathology image analysis. The code is available at <https://github.com/sagizty/CellMix>.

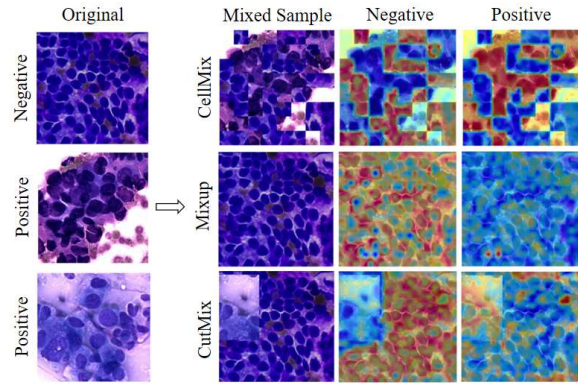


Figure 1. Visualization of an augmented example. Compared with other mixing-based methods, CellMix accurately identifies the boundary of patches and instances. It also tells the differences between negative and positive.

## 1. Introduction

Deep neural networks (DNNs) have shown impressive performance in pathology image analysis. However, this success crucially relies on the availability and quality of annotated pathology images, which are very difficult to collect and need lots of human effort. To alleviate this problem, data augmentation, which enlarges the amount and diversity of the labeled samples with label-preserving transformations, is a feasible method to improve the generalization of DNNs.

Data augmentation has been extensively established in the traditional computer vision field. Beyond the traditional preprocess data augmentation methods (including: rotate, flip, etc.), the mixing-based approach is one of the most representative methods. Mixing-based methods are domain-agnostic data augmentation techniques first proposed by

\*These authors contributed equally to this work.

Tianyi Zhang (zhangtianyi@buaa.edu.cn)

Zhiling Yan (zhilingyan724@outlook.com)

†Corresponding author.

Guanglei Zhang (guangleizhang@buaa.edu.cn)

[36]. It devises a strategy that mixes some sub-regions or features from different categories of images, as new pseudo samples. Specifically, Mixup [36], Cutout [4], and CutMix [35] apply the mixing process at the instance level. While Patchup [6] trims the hidden layers and mixes the image at the feature level. PuzzleMix [17] and SaliencyMix [31] first devise strategy to extract the salient instance of the original images, then establish the mixing process.

However, more than directly applying the existing mixing-based methods to pathology image analysis, the innovations are needed due to the following three reasons:

1. Domain characteristics of pathology images. According to our observation, there are three basic and essential pathology image characteristics in the pathology field. (1) Local specificity. Factors such as the size of cells, the ratio of the nucleus to the cytoplasm, and the distribution of cell chromatin are important components of pathology image features. They are often scattered in various parts of the image, requiring careful observation of local areas. (2) Global distribution characteristics. Factors such as the relative size of cells, the overall orientation of cells, and the consistency of cell spacing need to be analyzed as a whole for the entire image. (3) Inner/outer-sample instance relationship. In pathology images, there are different granularities of pathology instances in the same sample, such as cells, tissues, etc. Instances of the same category appear similar, while the relationship of different instances acts as the main feature. The relationship between instances in the same image, which is called the **inner-sample instance relationship**, is a discriminative element in lesion identification. Besides, the relationship across instances in different samples is called **outer-sample instance relationship**. Once we capture the proper outer relationship, we can combine the related instances into a meaningful pathology image. Therefore, we need a proper mixing approach as a data augmentation method that well models the inner-sample relationship and combine instances in proper outer-sample relationships to generate new images.

2. Perturbation information. Pathology images are artificially processed (stained/photographed), which inevitably introduces noise, leading to the inconsistency in the distribution of pathology images corresponding to the same label. In fact, the attention map in earlier pathology image analysis work always highlights some unrelated regions in the images [37], which also validates the impact of perturbation information. Therefore, it is much tougher to do the augmentation while preserving the labeling consistency.

3. Different data distribution between pathology images. In the pathology field, due to the difference in collection devices or preprocess methods during the pathology data collection process, a large gap exists between images under the same pathology task. Thus, previous mixing-based methods will intermingle a variety of different distribution infor-

mation, making the subsequent learning procedure harder. Therefore, we need a careful training strategy to reduce the difficulty in the learning process.

To address the three issues mentioned above, first, we propose a CellMix framework based on an in-place shuffle strategy to achieve the augmentation process.

Specifically, we split the images into patches and shuffle them in the same position across one batch at a certain proportion. We use the same proportion to blend the labels of these batch samples. This process is called the in-place shuffle strategy (illustrated in Figure 2). The patch size is designed to be consistent with the instance’s granularity, which contains local specificity. In this way, the inner/outer-sample instance relationships and global features in pathology images remain relatively stable compared to other methods. Therefore, we recreate newly labeled pathology samples via the shuffle procedure which complies with the characteristics of pathology images.

Second, inspired by the idea of curriculum learning [2], we devise a loss-drive strategy during the training process. Due to the perturbation noise and domain gap across the pathology images, it is a challenging task to directly use the aforementioned augmented data in the downstream training process. Curriculum learning imitates the learning process of human beings. It advocates that the model should learn from the easy samples, and gradually advance to the complex samples. It is proven to be very effective in dealing with complex tasks in numerous research [21, 24, 29, 34]. Therefore, in our CellMix framework, we design a fixed-position ratio scheduler and a patch-size scheduler towards the in-place shuffle process. We continuously change the patch size and the fixed-position ratio of pathology images to reduce the difficulty of the training task. In this way, we can gradually enhance the modeling ability towards biased pathology images and fit the domain gap adaptively. Furthermore, to make the training model control the schedule of learning process by itself, we devise a loss-drive ratio changing guideline. We judge the learning procedure by the loss of our model and alter the difficulty respectively, which is also a crucial approach to further improve the training efficiency.

In summary, our contribution can be concluded as the following four aspects:

1. We are the first to develop data augmentation techniques in pathology images and summarize three key issues in the augmentation process. These issues includes the characteristics in the pathology field, especially the relationship modeling and original noise in pathology images, which should be highly considered in the augmentation process.

2. We propose a CellMix framework based on an in-place shuffle strategy, which explicitly considers the characteristics of pathology images, especially the inner/outer instance relationship to do the data augmentation in a mixing-

based manner.

3. We devise a loss-drive curriculum learning strategy during training, making the training process adaptively to the augmented data.

4. The experiments conclude that our CellMix framework outperforms the previous SOTA method among 7 different datasets.

## 2. Related Work

### 2.1. Data Augmentation

Data augmentation has been widely used in deep learning models. Mixup [36] produces an augmented image by a pixel-wise weighted combination of two images. Cutout [4] proposes to mask fixed-size square regions of the input training images. CutMix [35] randomly masks a rectangular-shaped region of one image and replaces it with the corresponding position of another image. Patchup [6] and Manifold mixup [32] extend the concept of mixup from input space to hidden feature space. FMix [9] uses random-shape masks sampled from Fourier space. PuzzleMix [17], SaliencyMix [31] and Co-Mix [16] focus on image saliency analysis. The mask tries to reveal the most salient regions of images and maximize the saliency of the augmented image. ResizeMix [25] directly resizes the source image to a small patch and pastes it on another image. RandomMix [22] randomly selects a mixing sample data augmentation method from candidates, which increases the diversity of the mixed samples.

### 2.2. Curriculum Learning

Bengio et al. [2] proposed a new learning paradigm called curriculum learning (CL). In this strategy, a model is learned by gradually including from easy to complex samples in training in order to increase the entropy of training samples. Previous researches have proved that CL is consistent with the principle in human teaching [1, 15]. It often utilizes prior knowledge provided by instructors as guidance for curriculum design. It means that the predetermined curriculum heavily relies on the quality of prior knowledge while ignoring feedback about the learner.

To alleviate this issue, Kumar et al. [19] designed a new formulation, called self-paced learning (SPL). SPL adds a regularization term into the learning objective as the curriculum design. SPL leaves learners the freedom to adjust to the actual curriculum according to their learning paces. Various SPL-based applications have been proposed recently [12, 20, 30]. However, SPL is unable to deal with prior knowledge. Self-paced curriculum learning (SPCL) [13], as an “instructor-student-collaborative” learning mode, considers both prior knowledge and information learned during training, which gives inspiration to CellMix.

## 3. Method

In our CellMix framework for pathology image augmentation, there are two main components (demonstrated in Figure 2). First is the in-place shuffle strategy, which re-groups the patches in pathology images and generates augmented samples. Second is the loss-drive strategy, which includes a patch-size scheduler and a fix-position ratio scheduler driven by the model loss. This designation in curriculum learning aims to make the training process more effective and is flexible to deal with the pathology noise aforementioned. Besides, with the shift of patch-size and fix-position ratio, different scales of pathology image features are included. In this way, the curriculum learning process also makes the augmented pathology samples more representative. We will give a detailed description of the two main components in the following sections.

### 3.1. In-place Shuffle Strategy

The in-place shuffle strategy draws lessons from the idea of a mixing-based augmentation approach from the computer vision community. It holds the hypothesis that image labels preserve consistent visual information which can be mixed to generate interpolative samples. Besides, our in-place shuffle strategy highly considers the characteristics of the pathology field. Here we will introduce the main process of the in-place shuffle process.

Let  $I \in \mathbb{R}^{W \times H \times C}$  represent a pathology image, where  $W, H, C$  denote the width, height, and channel of the images respectively. Same with ViT, we first equally split the image into  $n$  patches, thus the image can be represented as

$$I = \{P_0, P_1, \dots, P_n\}, \quad P_i \in \mathbb{R}^{[p,p,C]}$$

where  $P_i$  denotes each patch, and we assign  $p$  to denote the patch size of  $P_i$ . Let  $B$  denote the batch in the training process. In our in-place shuffle strategy, we take  $\beta$  as the fix-position ratio. We randomly select  $m$  patches in the same position across one batch  $B$ :

$$m = n \times \beta, \quad \beta \in [0, 1]$$

which are regarded as position tokens  $F$  that do not participate in the shuffle process. And other patches are relation tokens  $R$ , acting as patches to be shuffled. By fixing a subset of patches unchanged, we preserve this part of inner-sample instance relationship, which is essential in pathology modeling.

Next, we do the in-place shuffle process. We shuffle the relation tokens across each batch  $B$  while keeping the position token fixed (illustrated in the right part of Figure 2) which can be formulated as:

$$P_{a,i} = M \odot P_{F,i} + (1 - M) \odot P_{R,i}, \quad i \in n$$

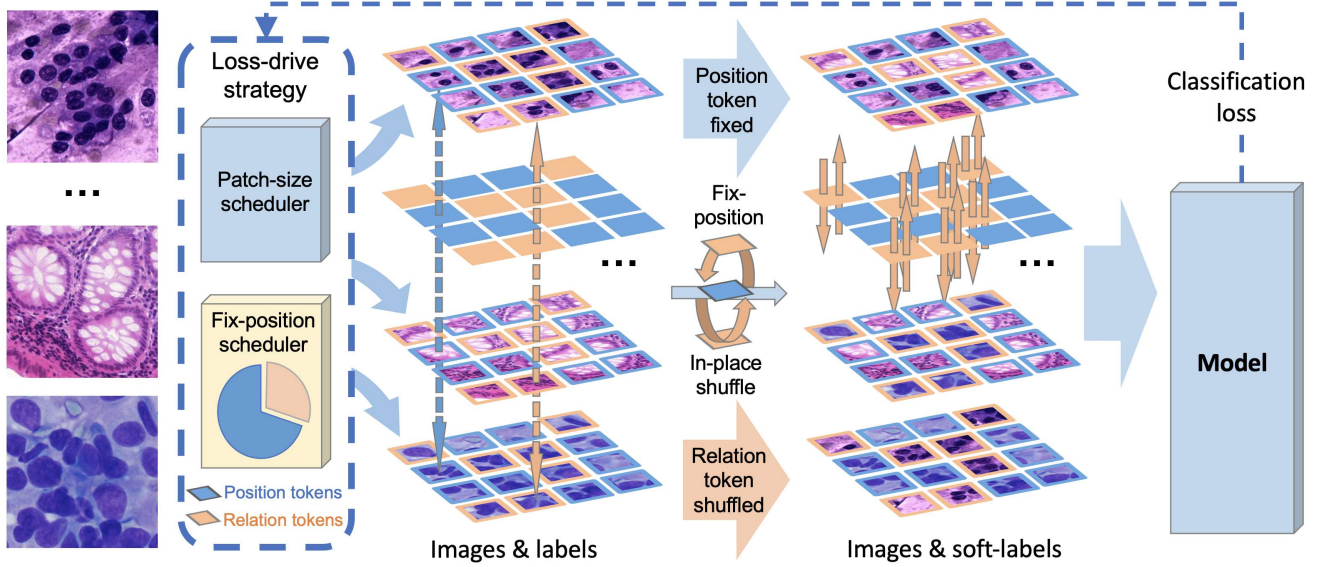


Figure 2. Overview of CellMix containing two components: In-place shuffle strategy and Loss-drive curriculum learning process. First, images are split into patches. Then in Fix-position in-place shuffle strategy, we randomly select position tokens that do not participate in the shuffle process, shown in blue. Yellow patches are relation tokens to be in-place shuffled. Next, in the right part of the figure, we shuffle relation tokens across the batch, remaining their relative positions the same in images. Soft labels are generated from ground truth labels according to the fix-position ratio. For the Loss-drive strategy in the blue box, we designed a Patch-size scheduler and Fix-position scheduler to adaptively guide the learning process according to the model loss. It is introduced specifically in Figure 3.

where  $\odot$  is element-wise multiplication and  $M$  denotes a binary mask, serving to assign the two kinds of tokens.

$$M = \begin{cases} 0, & i \in R \\ 1, & i \in F \end{cases}$$

In this way, we augment new pathology sample  $P_{a,i}$  through the shuffle process.

Meanwhile, the image labels need to be processed synchronously according to the fix-position ratio  $f$ . Considering that the image label is discrete, We need to use an interpolation method to derive the soft label of the enhanced sample:

$$y_a = f y_f + (1 - f) y_r, \quad y_a \in R^{[cls]}, \quad y_f, y_r \in I^{[cls]}$$

where,  $f \in (0, 1)$  denotes the mix-proportion,  $y_a$  denotes the soft label of augmented samples,  $y_f, y_r$  are one-hot vectors.  $y_f$  denotes the label of fix-position tokens and  $y_r$  denotes the relation tokens. The  $[cls]$  denotes the number of classification categories.

With our in-place shuffle strategy, the absolute relationship of the tokens remains, making the embedding of features fixed in the training process. In this way, compared to other methods, the important relative relationships and global features in pathology images remain stable. Therefore, we recreate pseudo samples via the shuffle procedure which complies with the characteristics of pathology images.

## 3.2. Loss-drive Curriculum Learning

Due to the influence of perturbation information of the pathology image and the inconsistency of data distribution, it is often difficult to directly use augmented samples for training downstream tasks. Inspired by the idea of curriculum learning, we imitate the process of human learning knowledge and design training courses from easy to difficult for the model.

### 3.2.1 Two Schedulers in Curriculum Learning

Specifically, in the in-place shuffle strategy, different patch sizes and fixed position ratios will affect the complexity of generated samples and bring about different training difficulties. At the same time, since pathology images actually contain features of different levels and scales, we also hope that the samples augmented by the shuffle process can be representative and flexible. In our framework, we design a patch-size scheduler and fix-position ratio scheduler, as shown in Figure 3.

With the patch-size scheduler, we continuously reduce the patch size in splitting the pathology images as follows:

$$[p_n, p_{n-1}, \dots, p_1], \quad p_n > p_{n-1} > \dots > p_1$$

During this process, we have more and more refined modeling of the relative relationship among instances.

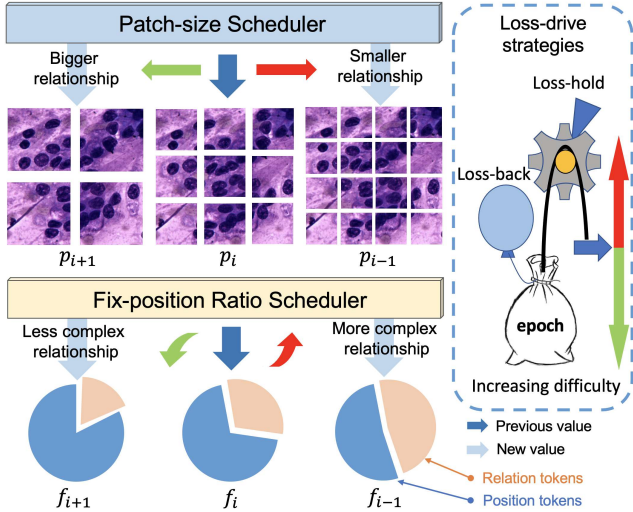


Figure 3. Structure of Loss-drive curriculum learning process. First, we design two schedulers: A Patch-size scheduler and a Fix-position scheduler. The former one schedules patch size from bigger to smaller, while the latter one gradually reduces the ratio of fix-position tokens (patches) in the shuffle process. Then, Loss-drive strategies, shown in the blue box, are proposed to determine how schedulers work. When the model learns well, we increase the difficulty as the red arrow. Otherwise, with the green arrow, the difficulty decreases. The curriculum remains the same in Loss-hold or steps backward to a simpler one in Loss-back.

From the big-scale relationship to the small-scale relationship, the augmented samples cover the relationship of different granularity.

In the fix-position ratio scheduler, we continuously reduce the fix-position ratio in the shuffle process as follows:

$$[f_n, f_{n-1}, \dots, f_1], \quad f_n > f_{n-1} > \dots > f_1, \quad f_i \in (0, 1)$$

In this way, the mixing efficiency of the in-place shuffle is constantly improved, and the pathological relationship is becoming more and more complex, making the model adaptively enhance the modeling ability.

Furthermore, in our curriculum learning, we do not learn the subset of total samples every epoch, but all samples with different patch sizes and fix-position ratios. In this way, we manage to plan the augmented pathology images to be trained for the model from easy to difficult. This process eliminates the influence of perturbations in the pathology field and improves the training effect and learning efficiency of augmented samples. At the same time, due to the change of schedule, the model can perceive the pathological characteristics across different scales. This training strategy makes the augmentation samples obtained by the in-place shuffle process become more representative.

### 3.2.2 Loss-drive Strategy

On the basis of the above patch size schedule and fixed position ratio schedule, we draw on the idea of self-paced curriculum learning and hope that the training model can adjust the schedule itself to control the learning process. To this end, we guide the learning process according to the model loss, as shown in the right half of Figure 3.

Specifically, in the training process, let the loss of the current iteration be  $l$ , and the learning threshold is  $T$ . When the loss value of the model is less than a certain threshold, the model has been learned well enough for the current course, which indicates the current course is simple enough for the model. Therefore, we increase the difficulty of the curriculum by reducing the patch size and diminishing the fix-position ratio.

$$p_i \rightarrow p_{i-1}; f_i \rightarrow f_{i-1} \quad \text{iff} \quad l < T$$

On the contrary, when the loss  $l$  is larger than the threshold  $T$ , we give two strategies to control the schedule. First, the loss-hold strategy, which make the schedule remain unchanged.

$$p_i \rightarrow p_i; f_i \rightarrow f_i \quad \text{iff} \quad l \geq T$$

Second, the loss-back strategy, which pushes back to the previous schedule.

$$p_i \rightarrow p_{i+1}; f_i \rightarrow f_{i+1} \quad \text{iff} \quad l \geq T$$

We will compare the two strategies in the experiments in Section 4. With loss-drive strategy, the model can adjust the difficulty by itself, so as to further improve the training efficiency of augmented samples.

## 4. Experiment

In this section, we mainly demonstrate the effectiveness, generalizability, and robustness of CellMix. To evaluate the performance of CellMix, we apply it to 7 different pathology image classification datasets: ROSE [37], pRCC [7], WBC [18], MARS<sup>1</sup>, GS [18], Warwick [28] and NCT [14]. The datasets are introduced in Section 4.1, covering different feature scales, dataset scales, and variety of pathology tasks. As an instance regrouping strategy, CellMix is compared with several mixing-based state-of-the-art data augmentation variants in Section 4.2. Designed for patch-based learning approaches, CellMix also verifies the generalizability onto a wide range of backbones (CNN-based, ViT-based and Hybrid) in Section 4.3. Different CellMix strategies are introduced in Section 4.4 to explore the design concepts. Interestingly, we examine the effect of curriculum design and feature scale with different prior knowledge in Section 4.5. Lastly, for better interpretability, we

<sup>1</sup><https://www.marsbigdata.com/competition/details?id=21078355578880>

Dataset	Category Numbers	Image Numbers	Organ/Tissue	Field
ROSE	2	5088	Pancreas	Cytopathology
pRCC	2	1417	Kidney	Histopathology
WBC	5	14514	Blood	Cytopathology
MARS	3	1770	Stomach	Histopathology
GS	2	700	Stomach	Histopathology
Warwick	2	165	Colon & Rectum	Histopathology
NCT	9	100000	Colon& Rectum	Histopathology

Table 1. Dataset description.

use Grad-CAM [26] to illustrate that CellMix obtains the most accurate attention area among models in Section 4.6.

#### 4.1. Datasets and Implementation Details

As a general approach, many datasets are explored. The overview can be found in Table 1. More details of datasets and implementation refer to Appendix A and Appendix B respectively.

#### 4.2. Comparison with State-of-the-art Methods

In this section, we provide a comprehensive comparison with many state-of-the-art mixing-based augmentation methods. We reproduce the state-of-the-art data augmentation methods [4, 9, 25, 31, 35, 36] with official codes and settings and compare them with the CellMix method. The baseline does not use any mixing-based data augmentation methods. We denote the experiments as Baseline, CutMix, Cutout, FMix, Mixup, ResizeMix, SaliencyMix, and CellMix in the experiment tables. Every online augmentation method is triggered by 50% chance in the training process. Specific details can be found in Appendix B.

Table 2 shows CellMix significantly outperforms all other mixing-based augmentation methods. On small-size datasets including GS and Warwick which are relatively simple, the majority of data augmentation methods perform well including CellMix. On medium-size datasets including ROSE, pRCC, WBC and MARS, CellMix yields a striking performance advancement up to 4.59% in accuracy and 6.14% in F1-score compared with Baseline, which largely outperforms other SOTA methods. In addition, CellMix can steadily boost the performance on large datasets such as NCT, by 1.47% for accuracy and 2.74% for F1-score.

#### 4.3. Generalizability

To verify the generalizability of CellMix, we examine various baseline models divided into three sets: CNN-based backbones, ViT-based backbones and Hybrid backbones. CNN-based backbones include VGG16, VGG19 [27], Resnet50 [10], Xception [3] and Mobilenetv3 [11]. ViT-based models, also considered as patch-learning-based models are ViT-base [5] and Swin-base [23]. Conformer [8], Crossformer [33] and ResNet50-ViT [5] are Hybrid backbones. Unless specified otherwise, the model imple-

mentation is based on official codes and minimal changes are made to hyperparameters of these backbones.

In Table 3, CellMix reveals great advantages on ViT-based models, with up to 4.59% and 1.43% improvements on ViT-base and Swin-base models respectively. CellMix cuts input images into non-overlapping patches, which perfectly encounters the patch-learning-based models without breaking the actual value of tokens. The CellMix introduces an instance (patch) regrouping strategy to enhance the tokens’ relationship modeling in the attention-based approaches. This may explain why CellMix performs especially well on patch-learning-based models. For CNN-based backbones and Hybrid backbones, the proposed method consistently boosts the variants in the range of 0.1% to 3.18%.

In short, Table 3 shows the considerable generalizability of CellMix, considering the improvements of CellMix on non-patch-learning-based methods, and especially striking performance on patch-learning-based models.

#### 4.4. Variants on Shuffle and Loss-Drive Strategy

CellMix mainly innovates with the fix-position in-place shuffle strategy and loss-drive method. In this section, we explore variants of both the in-place shuffle strategy and the loss-drive method. In the in-place shuffle strategy, a set of randomly selected patches are shuffled across the batch, remaining the relative positions the same in images. For the first strategy of CellMix-group, those alternative patches are from the same image. For the second strategy CellMix-split, each patch is replaced separately, making extremely complex instance groups. In this way, the augmented images, containing regions from various samples are more biased toward each instance rather than focusing on the same-sample relationship of the instances.

As for the loss-drive method, we have two variants denoted as Loss-hold and Loss-back. Loss drive is an “instructor-student-collaborative” learning mode considering both prior knowledge of the curriculum and feedback from learners. The specific curriculum in the next iteration is defined by the model performance of the current epoch. If model learns well, we increase the difficulty of learning. While if not, the curriculum remains the same in Loss-hold or steps backward to a simpler one in Loss-back. Therefore, the model can learn different feature scales in a more comprehensive way.

As shown in Table 4, all variants of CellMix can steadily boost the baseline performance on all benchmarks. And CellMix-group with Loss-hold strategy, as the best variant, lifts the accuracy of ViT up to a remarkable 4.59%. Other variants lift the baseline result up to 3.89%, 1.41% and 1.87% for CellMix-group-Loss-back, CellMix-split-Loss-hold and CellMix-split-Loss-back respectively. Although all variants are effective, CellMix-split may over-

Method	ROSE		pRCC		WBC		MARS		GS		Warwick		NCT	
	Acc	F1	Acc	F1	Acc	F1	Acc	F1	Acc	F1	Acc	F1	Acc	F1
Baseline	91.63	87.66	92.58	90.05	98.39	99.24	96.31	95.85	99.29	99.55	100.00	100.00	98.19	96.38
CutMix	91.93	88.15	95.41	93.66	98.80	99.45	96.59	96.25	100.00	100.00	100.00	100.00	99.61	98.83
Cutout	92.72	89.58	93.29	91.24	97.60	98.44	96.88	96.49	98.57	99.11	100.00	100.00	98.33	96.11
FMix	93.41	90.41	93.64	91.35	98.32	98.99	96.31	95.79	100.00	100.00	100.00	100.00	99.39	98.59
Mixup	93.80	90.94	93.29	90.55	97.42	98.44	96.88	96.55	100.00	100.00	97.50	97.62	99.46	98.76
ResizeMix	92.52	88.66	95.76	94.34	98.20	98.90	97.44	97.12	100.00	100.00	100.00	100.00	99.57	98.78
SaliencyMix	93.21	90.18	94.70	93.02	98.92	99.55	98.01	97.78	100.00	100.00	100.00	100.00	99.50	98.76
CellMix	<b>94.49</b>	<b>92.07</b>	<b>97.17</b>	<b>96.19</b>	<b>99.26</b>	<b>99.70</b>	<b>98.86</b>	<b>98.74</b>	<b>100.00</b>	<b>100.00</b>	<b>100.00</b>	<b>100.00</b>	<b>99.63</b>	<b>99.12</b>

Table 2. Accuracy and F1-score comparison with state-of-the-art mixing-based data augmentation methods on datasets including ROSE, pRCC, WBC, GS, Warwick, MARS and NCT. All counterpart methods are evaluated with ViT-base.

Model	ROSE		pRCC		WBC		MARS		GS		Warwick		NCT	
	Baseline	CellMix	Baseline	CellMix	Baseline	CellMix								
VGG16	91.44	90.85	86.22	<b>86.22</b>	98.36	<b>99.03</b>	96.59	<b>98.01</b>	99.29	<b>99.29</b>	96.25	<b>97.50</b>	98.06	<b>99.55</b>
VGG19	89.96	<b>91.63</b>	88.34	87.28	98.25	<b>98.94</b>	96.88	<b>97.73</b>	99.29	98.57	95.00	<b>97.50</b>	98.10	<b>99.55</b>
Resnet50	91.14	<b>91.24</b>	90.46	89.40	98.92	<b>98.50</b>	97.44	<b>97.73</b>	100.00	<b>100.00</b>	100.00	<b>100.00</b>	99.19	<b>99.67</b>
Xception	90.65	<b>90.85</b>	82.69	<b>85.87</b>	98.20	<b>98.46</b>	97.44	96.59	96.43	<b>98.57</b>	100.00	<b>100.00</b>	99.23	<b>99.64</b>
Mobilenetv3	87.30	86.02	75.27	71.38	97.21	<b>97.74</b>	96.02	<b>96.02</b>	96.43	<b>96.43</b>	95.00	93.75	98.87	<b>99.24</b>
ViT-base	91.63	<b>94.49</b>	92.58	<b>97.17</b>	98.39	<b>99.26</b>	96.31	<b>98.86</b>	99.29	<b>100.00</b>	100.00	<b>100.00</b>	98.19	<b>99.63</b>
Swin-base	92.22	<b>93.31</b>	92.23	<b>92.93</b>	98.89	98.36	96.59	<b>97.44</b>	97.86	<b>99.29</b>	100.00	<b>100.00</b>	97.20	<b>99.46</b>
Conformer	91.34	<b>92.62</b>	92.93	90.11	97.74	<b>98.43</b>	96.02	<b>97.44</b>	100.00	<b>100.00</b>	100.00	<b>100.00</b>	99.60	<b>99.60</b>
Crossformer	91.73	<b>92.91</b>	89.40	<b>89.40</b>	97.14	<b>98.39</b>	96.31	<b>97.44</b>	99.29	<b>99.29</b>	97.50	<b>100.00</b>	97.77	<b>99.43</b>
ResNet50-ViT	92.62	<b>92.72</b>	90.81	90.11	99.06	98.92	96.59	<b>98.01</b>	99.29	<b>99.29</b>	100.00	<b>100.00</b>	99.73	<b>99.82</b>

Table 3. CellMix can steadily boost a wide range of model variants including CNN-based, ViT-based, and Hybrid models on all classification benchmarks. Note that all hyperparameters within one dataset remain the same as Section 2.

Method	ROSE	pRCC	WBC	MARS	GS	Warwick	NCT
Baseline	91.63	92.58	98.39	96.31	99.29	100.00	98.19
Group-Hold	<b>94.49</b>	<b>97.17</b>	<b>99.26</b>	<b>98.86</b>	<b>100.00</b>	<b>100.00</b>	<b>99.63</b>
Group-Back	93.60	96.47	99.03	98.30	100.00	100.00	99.61
Split-Hold	92.91	93.99	98.82	97.44	100.00	100.00	99.57
Split-Back	93.50	93.64	98.27	98.01	100.00	100.00	99.55

Table 4. Accuracy of variants for in-place shuffle strategy and loss-drive method. Group and Split denotes the CellMix-group and CellMix-split strategies respectively. Hold means the proposed Loss-hold strategy, and Back means Loss-back strategy.

complicate the augmentation images and break the absolute relationship of instances, resulting in negative effects on the performance. Loss-hold is better than Loss-back considering the potential over-simplified curriculum in the Loss-back strategy. CellMix-group with Loss-hold strategy is the default strategy denoted as CellMix unless specified.

#### 4.5. Curriculum Variants

As mentioned in Section 3, patch size and fixed position ratio of samples represent the difficulty of the curriculum. With an adaptive curriculum, the model can perceive the pathology characteristics across different scales and eliminate the perturbation information of pathology images. The prior knowledge is the range, i.e. learning space, of both two variables. In this section, we ablate different prior knowledge choices to explore the effect of curriculum de-

Patch Size	ROSE	pRCC	WBC
16	93.90	94.70	98.50
32	94.09	94.70	98.76
48	93.50	<b>96.11</b>	<b>98.78</b>
64	<b>94.19</b>	95.05	98.71
96	94.00	95.05	98.20
128	93.31	95.05	98.78
192	92.81	95.05	98.27

Table 5. Curriculum variants for patch size fixed in the range of 16 to 192. Fix-position ratio scheduler remains the same.

sign and feature scale. We fix different initial values for patch size from 16 to 192 as well as fix position ratio from 0.5 to 0.9, shown in Table 5 and Table 7 respectively. In addition, we choose different patch size lists including [128, 64, 32, 16] and [196, 96, 48, 16], shown in Table 6.

In Table 5, CellMix performs the best with fix-patch size 64 on ROSE and 48 on pRCC and WBC, while too small or too large patch size shows poor performance. In fact, instances (i.e. cells, tissues, etc.) are sparsely distributed in the majority of pathology images. With a large patch size, it is more likely to generate augmented samples with misleading supervisory signals. While too small, instances are split into pieces resulting in the loss of semantic information. This result verifies the capability of instance-based shuffle strategy and supports our hypothesis that local (instance) specificity, such as characteristics of cells, plays an

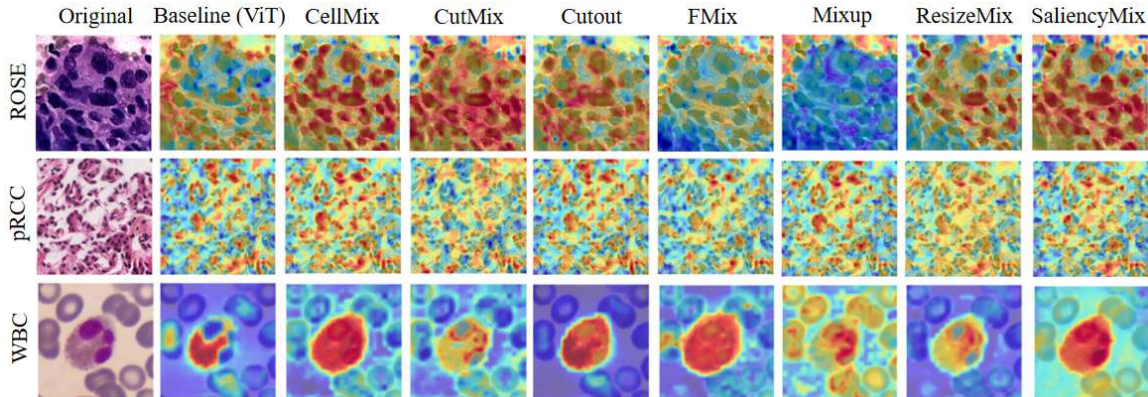


Figure 4. CAM visualizations on un-augmented images. The first column is the original image from ROSE, pRCC and WBC, and the other columns are Grad-CAM results. As shown in the figure, CellMix guides the model to precisely focus on target instances and can accurately recognize the contour of the cell area.

Patch Size	ROSE	pRCC	WBC
Even	93.70	96.47	98.62
Odd	94.19	95.76	98.32
Full	<b>94.49</b>	<b>97.17</b>	<b>99.26</b>

Table 6. Curriculum variants for different patch size lists. Full, as the default set, means patch size list [192, 128, 96, 64, 48, 32, 16]. Even is [128, 64, 32, 16], while Odd is [196, 96, 48, 16].

important role in modeling pathology image features.

Table 6 shows CellMix performs the best with a full patch size list. Specifically, it outperforms CellMix without full patch size lists in a range of 0.3% to 1.41%. Shortening the patch size list reduces learnable feature scales and the accuracy of results, which means a strategy with more comprehensive feature scales can work better in relationship modeling. In Table 7, CellMix with adaptive fix-position ratio outperforms others with given ratios from 0.13% to 2.82%. The drop in performance of the variant without a full patch size list and the variant without an adaptive fix-position ratio is consistent with the perspective that different feature scales contribute to better relationship modeling.

To further evaluate the loss-drive strategy with different loss thresholds and patch/ratio schedulers, more detailed ablation experiments are conducted in Appendix C.

#### 4.6. CAM Analysis

We extract Grad-CAM [26] for both un-augmented images and augmented images to investigate the regions of the input image where the model focuses to recognize an object.

Figure 4 shows that CellMix guides the model to precisely focus on the target object compared to other methods, presenting solid interpretability in cell identification. It shows that the model fully learns the feature of cell instances (local specificity) and the difference between in-

Fix Position Ratio	ROSE	pRCC	WBC
0.5	92.91	94.35	97.56
0.6	93.90	94.35	98.94
0.7	92.13	94.70	97.35
0.8	93.31	94.35	98.80
0.9	93.41	94.35	99.03
Adaptive	<b>94.49</b>	<b>97.17</b>	<b>99.26</b>

Table 7. Curriculum variants for given fix-position ratios. For example, 0.9 means 90% patches of one image are fixed in the in-place shuffle process, with 10% shuffled. Adaptive, as the default setting, represents the continuously decreasing fix-position ratio.

stances and background (global distribution).

We also visualize Grad-CAM on augmented images in Figure 1. It can be seen that CellMix effectively focuses on the corresponding features and precisely localizes the instances in the scene. Besides, it can be seen clearly that CellMix pays attention to different cells when making negative and positive predictions, and accurately identifies the boundary of different patches. It proves that CellMix indeed learns the difference between negative and positive instances and the inner/outer-sample instance relationship.

## 5. Conclusion

In conclusion, we introduce CellMix data augmentation method, which aims for the characteristics of pathology image analysis and forces the models to observe the relationship between the instances. We propose a distribution-based in-place shuffle strategy that can regroup patches (containing instances) in the image (bag) level, with two kinds of tokens assigned. At the image level, effective pseudo-samples force the models to observe the instance relationship. We devise a loss-drive curriculum learning strategy during the training process to cover the multiple potential feature scales and alter the modeling difficulty adaptively.

On various pathology image classification benchmarks, CellMix significantly outperforms all other mixing-based augmentation methods. CellMix boosts the performance of ViT-base model up to 4.59% in accuracy and 6.14% in F1-score. The inspiring SOTA results with various models prove the effectiveness of the core idea.

## 6. Acknowledgement

This work was partially supported by the National Natural Science Foundation of China (No. 62271023), the Beijing Natural Science Foundation (No. 7202102), and the Fundamental Research Funds for Central Universities.

## References

- [1] Sumit Basu and Janara Christensen. Teaching classification boundaries to humans. In *Proceedings of the AAAI Conference on Artificial Intelligence*, volume 27, pages 109–115, 2013. 3
- [2] Yoshua Bengio, Jérôme Louradour, Ronan Collobert, and Jason Weston. Curriculum learning (icml). *Google Scholar Google Scholar Digital Library Digital Library*, 2009. 2, 3
- [3] François Chollet. Xception: Deep learning with depthwise separable convolutions. In *Proceedings of the IEEE conference on computer vision and pattern recognition*, pages 1251–1258, 2017. 6
- [4] Terrance DeVries and Graham W Taylor. Improved regularization of convolutional neural networks with cutout. *arXiv preprint arXiv:1708.04552*, 2017. 2, 3, 6
- [5] Alexey Dosovitskiy, Lucas Beyer, Alexander Kolesnikov, Dirk Weissenborn, Xiaohua Zhai, Thomas Unterthiner, Mostafa Dehghani, Matthias Minderer, Georg Heigold, Sylvain Gelly, et al. An image is worth 16x16 words: Transformers for image recognition at scale. *arXiv preprint arXiv:2010.11929*, 2020. 6
- [6] Mojtaba Faramarzi, Mohammad Amini, Akilesh Badri-naaraayanan, Vikas Verma, and Sarath Chandar. Patchup: A regularization technique for convolutional neural networks. *arXiv preprint arXiv:2006.07794*, 2020. 2, 3
- [7] Zeyu Gao, Bangyang Hong, Xianli Zhang, Yang Li, Chang Jia, Jialun Wu, Chunbao Wang, Deyu Meng, and Chen Li. Instance-based vision transformer for subtyping of papillary renal cell carcinoma in histopathological image. In *International Conference on Medical Image Computing and Computer-Assisted Intervention*, pages 299–308. Springer, 2021. 5
- [8] Anmol Gulati, James Qin, Chung-Cheng Chiu, Niki Parmar, Yu Zhang, Jiahui Yu, Wei Han, Shibo Wang, Zhengdong Zhang, Yonghui Wu, et al. Conformer: Convolution-augmented transformer for speech recognition. *arXiv preprint arXiv:2005.08100*, 2020. 6
- [9] Ethan Harris, Antonia Marcu, Matthew Painter, Mahesan Niranjan, Adam Prügel-Bennett, and Jonathon Hare. Fmix: Enhancing mixed sample data augmentation. *arXiv preprint arXiv:2002.12047*, 2020. 3, 6
- [10] Kaiming He, Xiangyu Zhang, Shaoqing Ren, and Jian Sun. Deep residual learning for image recognition. In *Proceedings of the IEEE conference on computer vision and pattern recognition*, pages 770–778, 2016. 6
- [11] Andrew G Howard, Menglong Zhu, Bo Chen, Dmitry Kalenichenko, Weijun Wang, Tobias Weyand, Marco Andreetto, and Hartwig Adam. Mobilenets: Efficient convolutional neural networks for mobile vision applications. *arXiv preprint arXiv:1704.04861*, 2017. 6
- [12] Lu Jiang, Deyu Meng, Teruko Mitamura, and Alexander G Hauptmann. Easy samples first: Self-paced reranking for zero-example multimedia search. In *Proceedings of the 22nd ACM international conference on Multimedia*, pages 547–556, 2014. 3
- [13] Lu Jiang, Deyu Meng, Qian Zhao, Shiguang Shan, and Alexander G Hauptmann. Self-paced curriculum learning. In *Twenty-ninth AAAI conference on artificial intelligence*, 2015. 3
- [14] JN Kather, N Halama, and A Marx. 100,000 histological images of human colorectal cancer and healthy tissue (2018). DOI: <https://doi.org/10.5281/zenodo.1214456>, 2018. 5
- [15] Faisal Khan, Bilge Mutlu, and Jerry Zhu. How do humans teach: On curriculum learning and teaching dimension. *Advances in neural information processing systems*, 24, 2011. 3
- [16] Jang-Hyun Kim, Wonho Choo, Hosan Jeong, and Hyun Oh Song. Co-mixup: Saliency guided joint mixup with super-modular diversity. *arXiv preprint arXiv:2102.03065*, 2021. 3
- [17] Jang-Hyun Kim, Wonho Choo, and Hyun Oh Song. Puzzle mix: Exploiting saliency and local statistics for optimal mixup. In *International Conference on Machine Learning*, pages 5275–5285. PMLR, 2020. 2, 3
- [18] Zahra Mousavi Kouzehkanan, Sepehr Saghari, Sajad Tavakoli, Peyman Rostami, Mohammadjavad Abaszadeh, Farzaneh Mirzadeh, Esmail Shahabi Satsar, Maryam Gheidshahran, Fatemeh Gorgi, Saeed Mohammadi, et al. A large dataset of white blood cells containing cell locations and types, along with segmented nuclei and cytoplasm. *Scientific reports*, 12(1):1–14, 2022. 5
- [19] M Kumar, Benjamin Packer, and Daphne Koller. Self-paced learning for latent variable models. *Advances in neural information processing systems*, 23, 2010. 3
- [20] M Pawan Kumar, Haihem Turki, Dan Preston, and Daphne Koller. Learning specific-class segmentation from diverse data. In *2011 International Conference on Computer Vision*, pages 1800–1807. IEEE, 2011. 3
- [21] Fenglin Liu, Shen Ge, and Xian Wu. Competence-based multimodal curriculum learning for medical report generation. *arXiv preprint arXiv:2206.14579*, 2022. 2
- [22] Xiaoliang Liu, Furao Shen, Jian Zhao, and Changhai Nie. Randommix: A mixed sample data augmentation method with multiple mixed modes. *arXiv preprint arXiv:2205.08728*, 2022. 3
- [23] Ze Liu, Yutong Lin, Yue Cao, Han Hu, Yixuan Wei, Zheng Zhang, Stephen Lin, and Baining Guo. Swin transformer: Hierarchical vision transformer using shifted windows. In

- Proceedings of the IEEE/CVF International Conference on Computer Vision*, pages 10012–10022, 2021. 6
- [24] Jinliang Lu and Jiajun Zhang. Exploiting curriculum learning in unsupervised neural machine translation. *arXiv preprint arXiv:2109.11177*, 2021. 2
- [25] Jie Qin, Jiemin Fang, Qian Zhang, Wenyu Liu, Xingang Wang, and Xinggang Wang. Resizemix: Mixing data with preserved object information and true labels. *arXiv preprint arXiv:2012.11101*, 2020. 3, 6
- [26] Ramprasaath R Selvaraju, Michael Cogswell, Abhishek Das, Ramakrishna Vedantam, Devi Parikh, and Dhruv Batra. Grad-cam: Visual explanations from deep networks via gradient-based localization. In *Proceedings of the IEEE international conference on computer vision*, pages 618–626, 2017. 6, 8
- [27] Karen Simonyan and Andrew Zisserman. Very deep convolutional networks for large-scale image recognition. *arXiv preprint arXiv:1409.1556*, 2014. 6
- [28] Korsuk Sirinukunwattana, Josien PW Pluim, Hao Chen, Xiaojuan Qi, Pheng-Ann Heng, Yun Bo Guo, Li Yang Wang, Bogdan J Matuszewski, Elia Bruni, Urko Sanchez, et al. Gland segmentation in colon histology images: The glas challenge contest. *Medical image analysis*, 35:489–502, 2017. 5
- [29] Yixuan Su, Deng Cai, Qingyu Zhou, Zibo Lin, Simon Baker, Yunbo Cao, Shuming Shi, Nigel Collier, and Yan Wang. Dialogue response selection with hierarchical curriculum learning. *arXiv preprint arXiv:2012.14756*, 2020. 2
- [30] Kevin Tang, Vignesh Ramanathan, Li Fei-Fei, and Daphne Koller. Shifting weights: Adapting object detectors from image to video. *Advances in Neural Information Processing Systems*, 25, 2012. 3
- [31] AFM Uddin, Mst Monira, Wheemyung Shin, TaeChoong Chung, Sung-Ho Bae, et al. Saliencymix: A saliency guided data augmentation strategy for better regularization. *arXiv preprint arXiv:2006.01791*, 2020. 2, 3, 6
- [32] Vikas Verma, Alex Lamb, Christopher Beckham, Amir Najafi, Ioannis Mitliagkas, David Lopez-Paz, and Yoshua Bengio. Manifold mixup: Better representations by interpolating hidden states. In *International Conference on Machine Learning*, pages 6438–6447. PMLR, 2019. 3
- [33] Wenxiao Wang, Lu Yao, Long Chen, Binbin Lin, Deng Cai, Xiaofei He, and Wei Liu. Crossformer: A versatile vision transformer hinging on cross-scale attention. *arXiv preprint arXiv:2108.00154*, 2021. 6
- [34] Benfeng Xu, Licheng Zhang, Zhendong Mao, Quan Wang, Hongtao Xie, and Yongdong Zhang. Curriculum learning for natural language understanding. In *Proceedings of the 58th Annual Meeting of the Association for Computational Linguistics*, pages 6095–6104, 2020. 2
- [35] Sangdoon Yun, Dongyoon Han, Seong Joon Oh, Sanghyuk Chun, Junsuk Choe, and Youngjoon Yoo. Cutmix: Regularization strategy to train strong classifiers with localizable features. In *Proceedings of the IEEE/CVF international conference on computer vision*, pages 6023–6032, 2019. 2, 3, 6
- [36] Hongyi Zhang, Moustapha Cisse, Yann N Dauphin, and David Lopez-Paz. mixup: Beyond empirical risk minimization. *arXiv preprint arXiv:1710.09412*, 2017. 2, 3, 6
- [37] Tianyi Zhang, Youdan Feng, Yunlu Feng, Yu Zhao, Yanli Lei, Nan Ying, Zhiling Yan, Yufang He, and Guanglei Zhang. Shuffle instances-based vision transformer for pancreatic cancer rose image classification. *arXiv preprint arXiv:2208.06833*, 2022. 2, 5